

Geochemical changes across the Ordovician-Silurian transition on the Yangtze Platform, South China

YAN DeTian^{1,2†}, CHEN DaiZhao², WANG QingChen² & WANG JianGuo²

¹ Key Laboratory of Tectonics and Petroleum Resources, Ministry of Education, China University of Geosciences, Wuhan 430074, China;

² State Key Laboratory of Lithospheric Evolution, Institute of Geology and Geophysics, Chinese Academy of Sciences, Beijing 100029, China

The trace element and rare earth element (REE) variations across the Ordovician-Silurian succession are presented from two outcrop sections on the Yangtze Platform: the Nanbazi section, Guizhou Province, deposited in a shallow platform interior setting, and the Wangjiawan section, Hubei Province, deposited in a deeper basinal environment. Geochemical analysis of closely spaced samples through three intervals, the Wufeng, Guanyinqiao and Longmaxi, revealed vast palaeoceanographic changes. Some geochemical proxies, including Th/U, Ni/Co, V/Cr, and V/(V+Ni) ratios, together with sedimentary facies and biotic data, indicate that an anoxic condition on the most of the Yangtze Platform during the Wufeng and Longmaxi intervals, but an oxic condition during the Guanyinqiao time. The shift of the anoxic to the oxic environment during the Guanyinqiao time coincided with a global sea-level lowstand, in parallel with the global glaciation. The Longmaxian anoxic environment was a result of a global sea-level rise, which may be synchronized with a mainly catastrophic event in the latest Ordovician. Although the two sections generally show similar variation patterns of trace and REE concentrations and some element ratios, a minor difference occurs between the Wangjiawan and Nanbazi sections, likely reflecting a difference in depositional setting during the accumulation. Such an oceanic oxygen-level variation may add a useful constraint to the current arguments on the cause and consequence of the latest Ordovician mass extinction.

rare earth elements, trace elements, paleo-redox proxies, mass extinction, Ordovician-Silurian boundary, Yangtze Platform

The end-Ordovician was marked by two phases of extinction that coincided with the major sea-level changes associated with the development and demise of Gondwanan glaciation^[1,2]. The timing, the global occurrence and synchronism of the event, in terms of the standard Late Ordovician graptolite zones, have not been well established until recently^[3,4]. Two major phases of mass extinction are recognized to be near the bases of the graptolite *N. persculptus* and *N. extraordinarius-N. ojsuensis* zones, respectively^[5,6]. Numerous lines of evidence have been obtained from North America, Europe, China, and North Africa for the globally synchronous Ordovician-Silurian boundary mass extinction events^[1,2,6]. Several hypotheses have been proposed as

the cause of this particular geologic event, including changes in sea level^[7], temperature^[8], and paleoceanography^[9], reduction in habitat^[10], bolide impact^[11], and any of the above combinations^[3]. The ultimate cause of this event, however, is still highly controversial.

Although a catastrophic event appears to have occurred at the Ordovician-Silurian boundary, long-term changes in environmental conditions appear to have played a role as well. There is strong evidence for environmental deterioration throughout the Ordovician-

Received March 26, 2008; accepted July 10, 2008

doi: 10.1007/s11430-008-0143-z

†Corresponding author (email: yandetian@mail.igcas.ac.cn)

Supported by National Basic Research Program of China (Grant No. 2005CB422101)

Silurian boundary, which may have stressed marine ecosystems prior to the main extinction event^[12]. In this study, we present the results of chemostratigraphic analyses of two well-exposed continuous Ordovician-Silurian boundary sections with a complete graptolite sequence from the Yangtze Platform on the South China plate. The present high-resolution analysis of these sections using multiple chemostratigraphic proxies provides apparent evidence of large, high-frequency changes in seawater chemistry during the Late Ordovician and Early Silurian, and is helpful to the understanding for origins of the catastrophic events.

1 Geological setting

The Yangtze Platform was a part of the South China Plate, a palaeocontinent separated during the Early Palaeozoic from the two other major Chinese palaeocontinents, the Tarim Plate and the North China Plate^[13]. Most of the strata from the Upper Ordovician to the Lower Carboniferous are missing in the Tarim Plate and the North China Plate, however, they are widespread on the South China Plate^[3,14]. Cocks^[15] suggested that the South China Plate occupied a tropical or subtropical location along the western margin of the Gondwanan craton. The Yangtze Platform could be divided by Jiujiang Strait into two parts: the Upper Yangtze to the northwest, and the Lower Yangtze to the southeast^[6,16]. As old lands and uplifts expanded and coalesced in the Late Ordovician, the Yangtze Sea, especially the Upper Yangtze Sea, became largely enclosed, characterized by restricted, low-energy and anoxic bottom water condi-

tions^[6]. Based on biostratigraphic data of graptolites and conodonts, Chen et al.^[4] suggested the biozones of Late Ordovician and Early Silurian in South China, and their correlations with the biozones elsewhere around the world.

Biostratigraphically well-constrained sections from two different localities on the Yangtze Platform were chosen for chemostratigraphic studies. They are the Wangjiawan section at Yichang, Hubei Province and the Nanbazi section at Tongzi, Guizhou Province (Figure 1).

Wangjiawan, situated in the central part of the Yangtze Platform and represented the deep water environment during the Ordovician Period, is a classic study area for the Ordovician biota^[3-6]. Nanbazi, located on the southwest part of the Yangtze Platform and represented a shallower water environment, is very similar in depositional sequence to the Wangjiawan section. The sequences of two sections comprise three successive formations: Wufeng, Guanyinqiao and Longmaxi formations. The Wufeng and Longmaxi formations are mainly composed of black shales, whereas Guanyinqiao Formation is characterized by the argillaceous limestones. Vertical lithofacies changes are suggested to have been resulted from the eustatic fluctuations, in response to the growth and demise of the Late Ordovician ice sheet^[1,12]. The faunal associations in these two sections are dominated by graptolites, except in the Guanyinqiao Formation in which the benthic *Hirnantian* fauna occurs extensively. Figure 2 shows the biostratigraphic correlations between these two sections, adopting the fossil zonation of Chen et al.^[4]. The Guanyinqiao For-

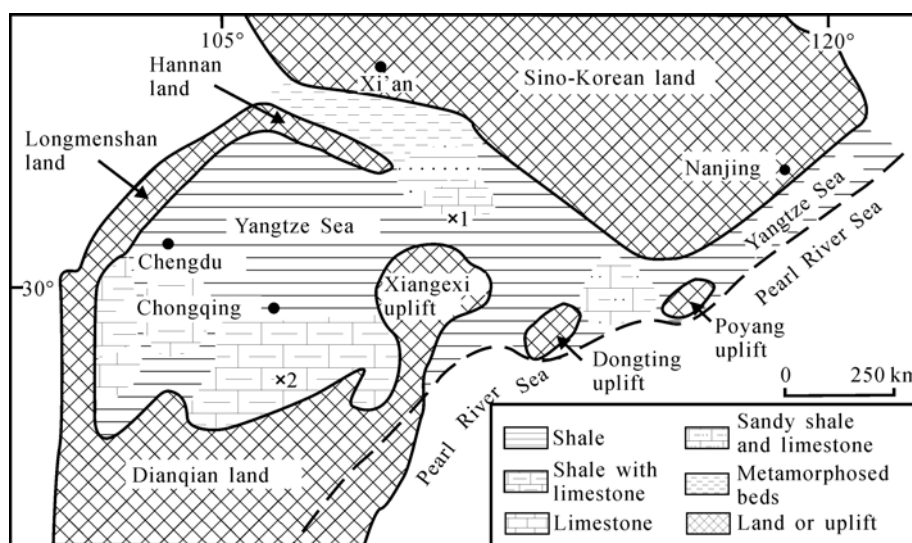


Figure 1 Late Ordovician paleogeography and facies map of the Yangtze Platform, South China^[6]. 1, Wangjiawan; 2, Nanbazi.

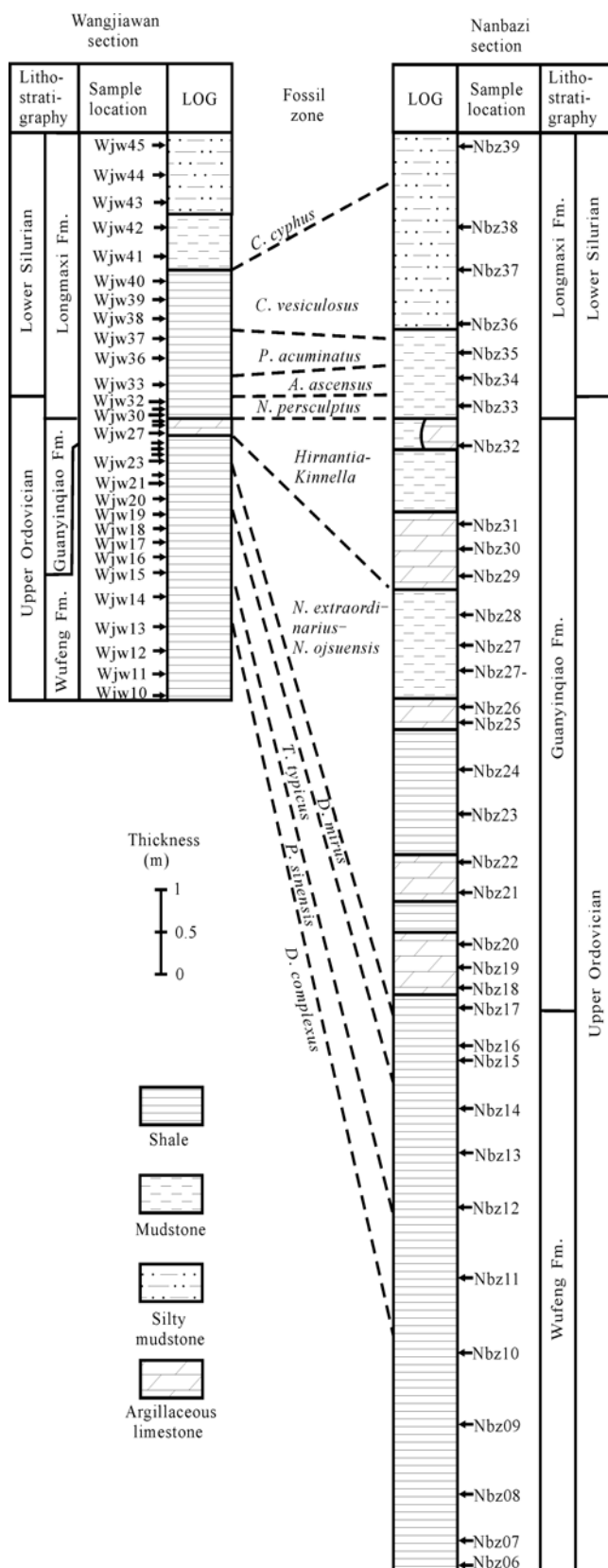


Figure 2 Lithological profiles of Wangjiawan section, Nanbazi section and their proposed correlation.

mation has been placed within the Wufeng Formation as a Member by others^[17], but its widespread distribution and distinctive character is appropriate for the “Formation” status^[18], applied in this study.

2 Samples and analytical methods

Sixty-nine samples were analysed, from the pre-glacial black shales in the Wufeng Formation through the glacial carbonate-rich Guanyinqiao Formation to the post-glacial black shales or silty mudstone of the Longmaxi Formation. Sampling positions are illustrated in Figure 2.

Prior to geochemical analyses, all fresh samples were crushed in the steel vessel and further ground to powder in an agate mill (200 mesh). The sample splits (100 mg) for element analysis were toasted in an oven at 105°C for 1–2 h and cooled to room temperature, then digested in a tightly sealed Teflon screw-cap beaker with ultrapure 0.5 mL HNO₃+2.5 mL HF+0.5 mL HClO₄, then dried. The dried sample was digested again with 1 mL HNO₃+3 mL H₂O until a clear solution was obtained. The solution was diluted to 1:1000 by mass and analyzed on a VG PQ2 Turbo inductively coupled plasma source mass spectrometer (ICP-MS) at the Institute of Geology and Geophysics, Chinese Academy of Sciences. Analytical precision for elemental concentrations was generally better than 4%.

Cerium (Ce/Ce^{*}) and europium anomalies (Eu/Eu^{*}) were calculated from: $Ce/Ce^* = Ce_n / (La_n \times Pr_n)^{1/2}$ and $Eu/Eu^* = Eu_n / (Sm_n \times Gd_n)^{1/2}$ ^[19], using shale-normalized abundances. Normalization values are a mean of North American, European and Russian shale composites^[20–22].

3 Results

3.1 Trace elements

Analytical results of trace elements are presented in Tables 1 and 2. Trace elements generally show systematic enrichment from the Wufeng Formation to Longmaxi Formation. A comparison of the average element compositions of multi-elements, normalized with the NASC standard, in different stratigraphic horizons shows that many elements such as V, Cr, Ni, Cu, Zn, Nb, Tl and Pb fluctuate in their abundance through time (Figure 3). Elements V, Ni, Cu, Zn, Ba, Hf, Ta, Tl and U are enriched relatively to the NASC standard in the Wufeng and Longmaxi formations, whereas other elements such

Table 1 REE and trace concentrations (ppm) of sedimentary rocks from the Wangjiawan section

Horizon	Wufeng Formation										
Sample	Wjw10	Wjw11	Wjw12	Wjw13	Wjw14	Wjw15	Wjw16	Wjw17	Wjw18	Wjw19	Wjw20
Li	21.83	20.17	18.69	17.77	28.42	22.85	15.27	13.50	36.21	16.77	21.63
Be	1.25	1.17	1.61	1.43	2.98	1.57	1.63	2.33	4.54	0.94	3.39
Sc	4.74	4.13	7.18	5.79	9.39	5.49	4.14	5.56	13.63	3.24	12.37
V	337.54	425.44	664.91	659.59	585.34	373.28	375.36	406.28	853.55	174.99	156.68
Cr	164.61	151.92	102.08	86.26	80.47	137.02	146.44	122.37	106.56	134.70	87.02
Co	4.50	3.56	6.79	3.42	9.53	8.22	6.61	11.24	16.15	7.20	15.85
Ni	49.83	44.20	91.68	53.24	82.20	80.62	81.66	137.87	187.48	70.16	65.16
Cu	44.64	35.08	88.41	58.73	53.77	52.00	64.01	56.65	130.09	32.92	112.82
Zn	100.47	51.09	50.78	39.15	258.46	191.62	71.30	249.57	249.49	119.35	66.88
Ga	6.16	6.77	10.14	8.38	19.00	8.61	9.20	11.43	21.35	4.27	16.91
Rb	44.49	42.88	73.12	60.44	97.46	53.31	56.90	79.39	139.20	31.15	121.14
Sr	40.94	40.10	47.03	42.92	55.02	41.38	39.39	43.05	60.19	40.51	55.52
Y	12.63	15.36	22.79	12.94	29.59	17.23	12.64	20.62	35.87	12.31	35.75
Zr	56.02	57.77	95.52	73.89	243.08	104.71	72.85	138.62	181.06	38.29	133.49
Nb	6.39	6.72	9.32	7.31	18.97	7.32	9.13	9.74	22.67	4.27	13.90
Cs	2.82	2.68	4.47	3.70	5.90	3.30	3.56	4.70	9.72	2.07	8.82
Ba	887.39	910.45	964.29	999.83	1153.44	946.10	855.63	954.63	1292.41	1011.76	1438.33
La	16.10	17.41	26.93	22.66	51.24	21.24	20.15	26.11	49.48	12.65	43.72
Ce	28.64	31.45	48.51	39.33	82.70	39.57	43.07	58.95	90.53	25.29	82.88
Pr	3.35	3.63	5.89	4.58	9.19	4.55	4.71	5.47	11.66	3.03	9.55
Nd	12.29	13.44	22.01	15.58	29.91	15.86	16.55	20.60	44.31	11.77	34.61
Sm	2.38	2.64	3.89	2.75	4.95	3.11	3.38	3.63	8.44	2.59	6.67
Eu	0.53	0.53	0.83	0.53	0.81	0.71	0.64	0.83	1.37	0.37	1.26
Gd	2.16	2.65	3.67	2.44	4.56	2.95	3.28	3.62	7.79	2.50	6.37
Tb	0.36	0.44	0.59	0.38	0.73	0.47	0.47	0.56	1.18	0.39	0.99
Dy	2.12	2.59	3.54	2.16	4.55	2.80	2.44	3.15	6.59	2.11	5.97
Ho	0.44	0.52	0.75	0.44	1.01	0.58	0.45	0.67	1.35	0.41	1.30
Er	1.26	1.42	2.09	1.24	2.86	1.60	1.20	1.87	3.62	1.05	3.55
Tm	0.19	0.21	0.32	0.19	0.44	0.24	0.18	0.29	0.55	0.16	0.52
Yb	1.29	1.32	2.11	1.25	2.87	1.50	1.10	1.81	3.46	0.96	3.29
Lu	0.20	0.20	0.32	0.19	0.45	0.23	0.16	0.28	0.54	0.14	0.51
Hf	1.34	1.28	2.38	1.83	5.00	2.16	1.79	2.90	5.11	0.92	3.68
Ta	0.36	0.34	0.70	0.50	1.23	0.43	0.50	0.65	2.80	0.26	1.01
Tl	0.67	0.69	2.59	1.60	2.08	1.70	2.10	2.31	4.59	1.24	3.30
Pb	11.64	11.64	31.94	14.83	16.86	13.05	16.42	15.20	27.11	8.03	33.02
Bi	0.18	0.16	0.25	0.23	0.29	0.20	0.24	0.25	0.47	0.12	0.48
Th	5.81	5.04	10.72	7.87	10.31	6.43	6.50	8.17	19.06	3.91	16.43
U	5.69	5.45	13.63	9.10	10.82	9.36	10.49	13.34	21.25	8.96	27.86
ΣREE	71.30	78.44	121.45	93.72	196.26	95.42	97.79	127.83	230.86	63.42	201.17
Ce/Ce*	0.85	0.86	0.84	0.84	0.82	0.87	0.96	1.07	0.82	0.89	0.88
Eu/Eu*	1.02	0.87	0.96	0.90	0.74	1.03	0.85	1.00	0.74	0.64	0.85
La _n /Yb _n	1.21	1.28	1.24	1.76	1.73	1.37	1.78	1.40	1.38	1.28	1.29
Ce/La	1.78	1.81	1.80	1.74	1.61	1.86	2.14	2.26	1.83	2.00	1.90
Th/U	1.02	0.93	0.79	0.86	0.95	0.69	0.62	0.61	0.90	0.44	0.59
V/Sc	71.22	103.05	92.64	113.88	62.35	68.04	90.71	73.09	62.62	54.09	12.66
V/Cr	2.05	2.80	6.51	7.65	7.27	2.72	2.56	3.32	8.01	1.30	1.80
V/(V+Ni)	0.87	0.91	0.88	0.93	0.88	0.82	0.82	0.75	0.82	0.71	0.71

(To be continued on the next page)

(Continued)

Horizon	Wufeng Formation						Guanyinqiao Formation			Longmaxi Formation	
	Sample	Wjw21	Wjw22	Wjw23	Wjw24	Wjw25	Wjw26	Wjw27	Wjw28	Wjw29	Wjw30
Li	16.24	14.93	17.67	18.83	2.18	17.37	10.02	4.73	10.71	18.56	22.09
Be	2.99	2.90	2.27	3.34	6.32	3.10	2.20	1.81	2.94	4.19	4.16
Sc	9.56	8.82	8.30	11.65	9.43	6.78	6.68	4.26	8.89	7.37	9.44
V	113.63	120.96	175.65	248.41	197.67	115.65	52.03	36.04	191.24	610.66	1085.44
Cr	61.29	72.39	112.64	94.45	64.08	115.46	66.86	113.98	101.11	159.74	152.74
Co	20.71	18.30	8.71	53.87	37.14	16.02	6.52	6.95	7.34	12.07	16.57
Ni	89.72	98.07	102.17	495.05	393.62	105.98	60.46	70.54	90.37	210.99	269.95
Cu	92.89	83.43	65.27	152.87	110.99	48.50	12.78	7.84	23.05	108.49	150.38
Zn	100.73	82.91	255.00	2060.41	526.83	104.78	93.14	91.93	159.13	404.05	559.08
Ga	12.57	10.65	10.69	22.27	29.23	14.91	7.32	5.09	8.86	19.39	20.71
Rb	87.23	72.05	70.63	85.39	149.70	89.64	41.76	28.42	57.89	120.38	125.66
Sr	159.23	215.41	118.25	361.58	132.44	116.61	399.47	453.21	380.14	72.08	65.26
Y	36.25	34.35	16.17	75.41	53.86	29.76	57.25	28.63	37.89	23.20	30.00
Zr	104.65	94.94	98.61	207.36	381.65	146.13	94.23	90.85	114.78	167.51	195.60
Nb	11.06	8.92	9.37	37.13	45.96	18.72	9.33	7.14	9.71	17.72	19.37
Cs	5.86	5.18	4.64	5.58	7.20	5.43	2.72	1.94	3.76	7.85	8.74
Ba	1231.82	2094.49	1052.15	1604.49	4859.68	1215.99	1872.33	1280.24	1714.46	1295.76	1357.85
La	34.11	31.18	18.60	75.35	103.93	34.56	35.74	20.89	33.48	39.35	43.09
Ce	64.97	60.29	30.10	158.78	219.89	70.02	61.65	37.79	57.35	70.38	79.64
Pr	7.71	7.04	3.20	21.06	25.01	8.45	7.67	4.75	7.34	8.37	9.79
Nd	29.95	25.05	11.13	86.14	87.39	30.51	29.67	19.69	28.47	29.28	35.66
Sm	5.83	5.09	2.02	19.13	15.68	6.08	6.14	4.14	5.80	5.39	6.36
Eu	1.19	1.14	0.43	2.44	1.64	0.84	1.18	1.05	1.36	0.97	1.23
Gd	5.95	5.51	2.00	18.51	12.55	5.79	6.87	4.12	5.95	4.92	6.11
Tb	0.90	0.84	0.34	3.03	1.96	0.89	1.20	0.66	0.95	0.76	0.91
Dy	5.41	5.06	2.12	17.43	11.29	5.25	8.14	3.87	5.86	4.12	5.23
Ho	1.12	1.06	0.48	3.39	2.36	1.07	1.76	0.86	1.25	0.85	1.11
Er	3.25	3.07	1.48	8.33	6.70	3.22	5.23	2.27	3.36	2.35	2.85
Tm	0.48	0.47	0.28	1.12	1.00	0.48	0.82	0.33	0.50	0.36	0.41
Yb	3.04	2.99	2.06	6.81	6.42	2.98	5.22	2.07	3.22	2.27	2.70
Lu	0.49	0.44	0.35	1.01	0.92	0.44	0.81	0.32	0.49	0.33	0.38
Hf	2.65	2.38	2.64	6.09	13.39	4.25	2.37	2.44	3.01	4.94	5.02
Ta	1.02	0.74	0.69	2.75	6.19	1.11	0.54	0.38	0.62	1.59	1.59
Tl	2.02	1.29	2.11	32.31	18.33	1.06	0.41	0.51	1.70	5.23	5.02
Pb	28.90	17.19	11.17	46.61	57.37	21.64	10.52	8.04	10.57	27.94	25.19
Bi	0.32	0.30	0.25	0.93	1.56	0.33	0.15	0.10	0.17	0.42	0.40
Th	10.66	8.50	8.82	21.13	44.59	11.92	7.13	5.26	9.45	17.05	14.60
U	16.35	11.57	5.22	42.64	88.22	15.94	20.83	10.05	26.72	27.59	51.47
ΣREE	164.39	149.21	74.59	422.52	496.74	170.57	172.11	102.80	155.37	169.70	195.46
Ce/Ce*	0.87	0.89	0.84	0.87	0.94	0.89	0.81	0.83	0.80	0.84	0.84
Eu/Eu*	0.89	0.95	0.95	0.57	0.51	0.62	0.80	1.11	1.02	0.83	0.86
La _n /Yb _n	1.09	1.01	0.87	1.07	1.57	1.13	0.66	0.98	1.01	1.68	1.54
Ce/La	1.90	1.93	1.62	2.11	2.12	2.03	1.73	1.81	1.71	1.79	1.85
Th/U	0.65	0.73	1.69	0.50	0.51	0.75	0.34	0.52	0.35	0.62	0.28
V/Sc	11.89	13.71	21.16	21.32	20.96	17.07	7.79	8.45	21.51	82.82	115.01
V/Cr	1.85	1.67	1.56	2.63	3.08	1.00	0.78	0.32	1.89	3.82	7.11
V/(V+Ni)	0.56	0.55	0.63	0.33	0.33	0.52	0.46	0.34	0.68	0.74	0.80

(To be continued on the next page)

(Continued)

Horizon	Longmaxi Formation											
Sample	Wjw32	Wjw33	Wjw36	Wjw37	Wjw38	Wjw39	Wjw40	Wjw41	Wjw42	Wjw43	Wjw44	Wjw45
Li	24.59	26.29	19.14	19.47	16.42	10.60	13.97	17.33	14.56	5.66	11.83	9.35
Be	4.20	4.13	3.25	2.39	2.19	3.58	3.23	2.23	3.17	1.94	2.55	2.83
Sc	9.35	10.53	7.24	4.16	5.11	5.73	5.88	7.13	8.02	3.40	5.21	6.10
V	1063.25	1074.90	315.26	124.51	124.58	208.35	193.82	192.35	232.49	189.74	185.29	218.69
Cr	149.28	135.73	92.31	103.17	98.80	108.73	108.41	116.16	127.39	69.83	128.17	111.48
Co	21.76	23.20	16.81	61.07	11.64	13.00	23.41	9.47	16.20	6.20	13.39	12.65
Ni	304.76	330.05	236.66	377.95	107.14	114.55	156.85	87.22	132.70	56.47	127.17	118.48
Cu	96.31	107.06	53.93	69.63	34.28	47.32	51.30	43.84	75.96	40.75	59.08	62.61
Zn	563.78	485.76	209.92	710.98	87.06	83.73	253.62	40.91	79.13	29.24	112.29	103.83
Ga	18.22	18.72	12.21	9.55	12.49	15.07	11.69	10.82	16.01	9.46	11.13	14.16
Rb	115.31	116.98	71.46	50.64	51.45	75.55	68.52	61.10	94.20	64.43	72.63	88.06
Sr	61.29	63.06	53.02	53.49	45.27	48.76	46.02	46.40	59.24	43.58	46.32	63.06
Y	36.03	37.87	25.89	31.26	26.52	20.20	31.80	20.45	29.88	9.03	18.01	24.11
Zr	260.64	270.74	173.21	192.44	316.26	225.49	194.18	119.87	194.40	116.34	127.24	200.59
Nb	22.99	22.95	17.28	32.37	31.78	39.30	25.21	12.75	17.09	11.10	12.38	18.12
Cs	8.33	8.46	4.65	2.49	3.21	4.28	4.25	4.05	6.51	4.50	4.79	6.02
Ba	1263.06	1385.37	1411.95	2239.55	1230.09	1723.16	1033.50	998.90	991.00	1062.35	982.87	1536.13
La	46.65	46.73	37.19	41.44	45.80	48.44	35.40	26.63	41.55	20.94	28.06	36.81
Ce	84.79	83.59	69.63	82.71	84.80	98.77	72.49	55.70	79.56	46.06	58.70	77.41
Pr	10.75	10.92	8.54	10.53	9.89	11.06	8.66	6.17	9.59	4.36	6.62	8.65
Nd	40.72	42.33	31.87	40.46	36.12	41.63	33.73	22.98	35.03	13.69	23.12	30.02
Sm	7.61	7.72	5.97	8.15	6.76	7.23	7.25	4.66	6.85	2.39	4.56	5.72
Eu	1.37	1.46	1.03	1.43	1.32	1.22	1.36	0.96	1.44	0.37	1.02	1.13
Gd	7.26	7.56	5.58	7.61	6.08	6.03	6.89	4.11	6.43	2.01	4.14	5.16
Tb	1.12	1.15	0.88	1.16	0.90	0.81	1.04	0.65	0.95	0.29	0.61	0.77
Dy	6.49	6.63	4.76	6.06	5.17	4.12	5.78	3.60	5.26	1.61	3.30	4.19
Ho	1.31	1.38	0.94	1.17	1.06	0.79	1.19	0.76	1.09	0.32	0.65	0.87
Er	3.46	3.69	2.71	2.95	2.69	2.07	3.04	2.07	2.89	0.93	1.75	2.35
Tm	0.52	0.54	0.39	0.42	0.39	0.30	0.42	0.32	0.42	0.15	0.25	0.35
Yb	3.32	3.64	2.58	2.69	2.57	1.97	2.68	2.14	2.70	0.99	1.63	2.27
Lu	0.51	0.54	0.38	0.41	0.39	0.28	0.38	0.31	0.41	0.15	0.24	0.33
Hf	5.12	5.04	4.45	4.33	6.42	7.13	4.60	3.07	5.39	3.09	3.48	5.45
Ta	1.59	1.61	1.15	1.53	1.39	3.78	1.41	1.02	1.71	0.86	1.08	1.62
Tl	6.21	6.56	4.64	19.05	2.88	3.63	3.39	2.05	2.85	1.88	2.12	2.55
Pb	26.99	33.48	23.77	64.41	19.27	21.48	19.65	15.29	21.83	14.58	18.28	20.15
Bi	0.41	0.43	0.35	1.69	0.30	0.40	0.39	0.28	0.44	0.31	0.31	0.40
Th	15.85	15.97	13.45	13.07	11.56	15.70	13.10	11.08	15.69	9.21	10.89	14.51
U	46.72	52.49	42.47	44.24	20.38	22.33	18.56	11.97	22.71	11.14	15.35	19.56
ΣREE	215.86	217.86	172.46	207.19	203.93	224.71	180.30	131.04	194.16	94.25	134.65	176.00
Ce/Ce*	0.82	0.81	0.85	0.86	0.87	0.93	0.90	0.95	0.87	1.05	0.94	0.94
Eu/Eu*	0.81	0.84	0.79	0.80	0.90	0.81	0.84	0.96	0.95	0.74	1.03	0.91
La _n /Yb _n	1.36	1.24	1.40	1.49	1.73	2.39	1.28	1.20	1.49	2.06	1.67	1.57
Ce/La	1.82	1.79	1.87	2.00	1.85	2.04	2.05	2.09	1.91	2.20	2.09	2.10
Th/U	0.34	0.30	0.32	0.30	0.57	0.70	0.71	0.93	0.69	0.83	0.71	0.74
V/Sc	113.74	102.05	43.57	29.92	24.36	36.38	32.97	26.99	29.00	55.83	35.60	35.86
V/Cr	7.12	7.92	3.42	1.21	1.26	1.92	1.79	1.66	1.83	2.72	1.45	1.96
V/(V+Ni)	0.78	0.77	0.57	0.25	0.54	0.65	0.55	0.69	0.64	0.77	0.59	0.65

Table 2 REE and trace concentrations (ppm) of sedimentary rocks from the Nanbazi section

Horizon	Wufeng Formation										
Sample	Nbz06	Nbz07	Nbz08	Nbz09	Nbz10	Nbz11	Nbz12	Nbz13	Nbz14	Nbz15	Nbz16
Li	13.50	12.79	11.91	12.59	7.64	12.78	12.53	14.81	13.24	8.98	22.46
Be	2.46	2.18	1.71	1.71	1.70	1.79	2.17	2.09	2.52	3.00	3.53
Sc	7.78	10.48	7.88	7.23	4.20	7.97	6.16	9.56	8.19	6.46	12.38
V	1334.24	910.10	743.50	793.82	691.83	800.77	795.97	831.77	456.18	146.57	153.88
Cr	154.55	109.92	91.47	93.36	108.78	99.19	99.08	99.81	96.27	100.94	88.15
Co	4.63	3.83	3.58	5.04	5.25	4.65	6.06	6.26	8.55	16.15	24.02
Ni	134.35	79.62	87.94	74.46	85.17	79.54	89.32	85.95	97.16	75.00	104.85
Cu	95.57	45.48	42.91	62.67	72.14	53.41	81.84	69.89	96.46	98.04	121.53
Zn	216.62	160.16	152.52	108.32	138.23	162.24	120.96	142.24	87.15	53.15	75.65
Ga	13.69	14.02	10.06	9.03	8.56	10.37	9.61	11.67	12.99	14.41	17.73
Rb	116.84	119.79	89.63	81.78	75.51	91.35	79.64	104.90	102.20	105.22	131.43
Sr	51.25	51.74	50.98	45.11	40.88	43.68	38.20	49.19	42.25	64.05	82.06
Y	22.09	33.95	25.30	21.55	10.34	23.41	20.86	21.51	21.60	25.85	41.69
Zr	133.71	164.59	93.84	81.05	90.88	90.02	94.96	102.64	129.66	148.61	187.93
Nb	11.04	18.43	7.87	7.79	10.02	8.16	8.07	8.99	10.11	11.65	13.44
Cs	6.95	7.83	5.03	4.14	4.35	5.57	4.38	6.52	5.99	7.62	9.30
Ba	364.79	344.28	303.31	283.98	254.51	278.93	253.85	300.71	317.16	598.09	1280.80
La	32.54	36.84	27.39	24.34	20.08	27.17	26.89	29.45	29.59	34.94	44.36
Ce	58.36	62.93	45.92	43.14	40.80	47.46	46.38	50.47	51.37	72.05	88.80
Pr	6.97	7.51	5.84	5.32	4.27	5.71	5.99	5.91	6.22	7.60	10.53
Nd	24.72	27.23	22.24	19.48	14.17	21.19	22.83	20.49	22.97	27.83	41.66
Sm	4.59	4.63	3.95	3.65	2.59	4.06	4.31	3.63	4.19	5.34	7.99
Eu	0.82	0.85	0.73	0.67	0.46	0.72	0.74	0.70	0.81	1.03	1.44
Gd	4.14	4.70	3.88	3.55	2.32	3.93	3.95	3.36	3.67	4.93	7.51
Tb	0.65	0.77	0.66	0.58	0.35	0.64	0.62	0.55	0.61	0.76	1.22
Dy	3.73	4.89	3.88	3.49	1.87	3.71	3.64	3.38	3.82	4.60	7.02
Ho	0.78	1.10	0.82	0.74	0.38	0.79	0.77	0.73	0.82	0.97	1.49
Er	2.11	3.27	2.34	2.02	1.02	2.19	2.07	2.09	2.43	2.70	4.13
Tm	0.31	0.50	0.36	0.31	0.16	0.33	0.31	0.33	0.37	0.41	0.60
Yb	2.00	3.29	2.32	2.03	1.01	2.20	1.99	2.17	2.50	2.75	3.96
Lu	0.30	0.51	0.36	0.31	0.15	0.33	0.29	0.33	0.37	0.42	0.61
Hf	3.53	3.55	2.44	2.16	2.34	2.39	2.58	2.80	3.51	4.01	5.34
Ta	1.05	0.82	0.61	0.59	0.60	0.61	0.65	0.70	1.02	1.00	1.01
Tl	0.87	0.97	0.81	0.63	0.74	1.08	0.70	1.00	1.10	1.84	1.96
Pb	16.43	30.07	13.61	9.08	9.30	13.55	11.21	13.73	19.45	27.18	32.01
Bi	0.36	0.29	0.26	0.22	0.24	0.27	0.26	0.30	0.32	0.36	0.37
Th	13.17	12.10	10.16	8.95	8.00	9.77	9.95	11.10	12.93	13.35	15.99
U	17.18	15.75	11.50	8.57	7.83	9.38	9.65	9.16	16.12	18.87	17.36
ΣREE	142.02	159.01	120.69	109.62	89.61	120.41	120.78	123.59	129.75	166.31	221.30
Ce/Ce*	0.84	0.82	0.79	0.83	0.96	0.83	0.80	0.83	0.83	0.96	0.89
Eu/Eu*	0.83	0.80	0.82	0.82	0.83	0.79	0.79	0.88	0.91	0.88	0.82
La _n /Yb _n	1.57	1.09	1.14	1.16	1.93	1.20	1.31	1.31	1.15	1.23	1.08
Ce/La	1.79	1.71	1.68	1.77	2.03	1.75	1.72	1.71	1.74	2.06	2.00
Th/U	0.77	0.77	0.88	1.04	1.02	1.04	1.03	1.21	0.80	0.71	0.92
V/Sc	171.52	86.82	94.31	109.84	164.80	100.51	129.20	86.98	55.69	22.69	12.43
V/Cr	8.63	8.28	8.13	8.50	6.36	8.07	8.03	8.33	4.74	1.45	1.75
V/(V+Ni)	0.91	0.92	0.89	0.91	0.89	0.91	0.90	0.91	0.82	0.66	0.59

(To be continued on the next page)

(Continued)

Horizon	Guanyinqiao Formation											
Sample	Nbz17	Nbz18	Nbz19	Nbz20	Nbz21	Nbz22	Nbz23	Nbz24	Nbz25	Nbz26	Nbz27-	Nbz27
Li	15.48	12.12	13.43	15.29	13.50	14.95	14.19	17.58	6.03	11.96	22.94	20.33
Be	2.33	1.26	1.75	1.41	2.06	2.10	2.10	2.41	0.68	1.39	2.79	2.36
Sc	8.67	4.74	5.83	5.90	8.09	7.83	8.34	10.96	2.19	6.30	12.36	11.82
V	112.11	73.29	49.76	42.39	52.40	56.63	45.22	96.47	34.16	64.30	130.45	113.79
Cr	60.65	34.98	78.43	50.44	44.51	55.56	111.47	84.73	16.68	15.50	81.16	65.92
Co	14.26	9.23	5.30	4.36	4.14	4.41	4.94	5.02	6.00	9.44	13.62	9.48
Ni	72.07	61.37	44.81	30.39	19.48	23.86	49.95	35.51	15.51	30.86	54.04	32.33
Cu	82.29	47.63	32.44	32.74	20.28	22.75	33.70	41.76	7.92	11.43	27.97	16.38
Zn	40.90	15.77	36.11	35.38	102.59	53.82	71.96	92.30	39.43	100.39	86.89	42.04
Ga	11.55	5.64	8.14	8.68	14.73	13.54	14.42	14.14	2.91	7.68	16.29	14.27
Rb	86.55	38.24	64.97	62.06	110.62	105.67	110.49	126.52	25.21	65.28	148.21	143.15
Sr	282.42	569.65	359.29	263.49	217.97	223.80	270.92	185.99	711.57	643.44	229.38	275.62
Y	29.49	19.54	32.04	35.90	39.67	41.05	40.53	41.31	17.98	48.64	24.95	28.13
Zr	130.54	74.96	133.63	122.23	173.93	178.63	200.73	215.20	22.28	60.38	147.11	131.97
Nb	9.14	4.77	6.35	7.18	12.62	12.14	13.36	13.34	2.98	6.05	14.92	13.23
Cs	5.93	2.57	3.87	3.72	6.52	6.00	7.02	7.55	1.62	3.84	9.75	8.68
Ba	222.71	141.37	229.92	222.09	266.34	269.73	289.22	305.80	220.49	190.00	320.19	291.22
La	30.14	16.51	30.52	28.41	45.20	42.51	48.55	44.56	18.61	45.75	36.69	37.99
Ce	59.62	32.05	52.36	49.12	84.78	79.31	88.84	81.85	25.89	84.17	62.80	67.78
Pr	6.99	3.82	7.06	6.15	10.63	9.80	11.85	10.58	3.25	12.51	7.61	7.95
Nd	26.12	14.46	27.99	24.19	40.69	37.89	45.50	41.31	11.70	49.29	27.55	29.70
Sm	5.16	2.98	5.26	4.98	8.19	7.64	8.52	7.91	2.28	9.29	4.71	5.34
Eu	0.95	0.56	1.21	0.79	0.76	0.81	1.07	1.12	0.67	2.15	0.84	0.93
Gd	5.05	3.03	5.40	5.48	7.70	7.32	8.00	7.39	2.14	9.38	4.54	4.97
Tb	0.82	0.50	0.81	0.92	1.29	1.23	1.25	1.18	0.34	1.38	0.70	0.80
Dy	4.79	2.98	4.59	5.51	7.47	7.23	7.40	6.89	2.11	7.92	4.15	4.48
Ho	1.03	0.63	0.98	1.16	1.55	1.52	1.52	1.43	0.46	1.51	0.85	0.94
Er	2.85	1.79	2.54	3.09	4.26	4.10	4.02	3.91	1.25	3.68	2.41	2.56
Tm	0.43	0.28	0.36	0.44	0.63	0.60	0.57	0.57	0.19	0.45	0.37	0.38
Yb	2.78	1.79	2.17	2.67	4.09	3.71	3.59	3.63	1.18	2.55	2.41	2.43
Lu	0.42	0.27	0.32	0.40	0.60	0.55	0.54	0.55	0.17	0.35	0.35	0.36
Hf	3.52	1.98	3.64	3.38	5.44	5.57	6.33	6.46	0.60	1.71	4.23	3.86
Ta	0.64	0.33	0.54	0.49	1.06	1.04	1.58	1.05	0.19	0.50	1.44	0.99
Tl	1.80	0.82	0.58	0.44	0.89	0.73	0.96	0.90	0.31	0.51	1.10	0.85
Pb	22.52	11.52	17.20	13.19	20.08	18.36	20.56	20.74	8.86	11.73	15.80	15.96
Bi	0.24	0.13	0.08	0.10	0.30	0.24	0.30	0.23	0.08	0.13	0.28	0.25
Th	10.35	5.40	8.41	8.24	17.23	17.52	18.95	17.27	2.77	6.34	14.95	12.73
U	11.63	9.38	2.31	2.30	4.12	3.81	4.67	4.33	2.22	2.56	3.23	2.39
ΣREE	147.13	81.65	141.56	133.30	217.84	204.20	231.23	212.88	70.23	230.38	155.98	166.60
Ce/Ce*	0.89	0.88	0.78	0.81	0.84	0.85	0.81	0.82	0.73	0.77	0.82	0.85
Eu/Eu*	0.82	0.82	0.99	0.67	0.42	0.48	0.57	0.64	1.34	1.01	0.79	0.79
La _n /Yb _n	1.05	0.89	1.36	1.03	1.07	1.11	1.31	1.19	1.52	1.74	1.48	1.52
Ce/La	1.98	1.94	1.72	1.73	1.88	1.87	1.83	1.84	1.39	1.84	1.71	1.78
Th/U	0.89	0.58	3.64	3.58	4.18	4.60	4.06	3.99	1.25	2.48	4.63	5.32
V/Sc	12.94	15.45	8.53	7.18	6.47	7.24	5.42	8.80	15.58	10.20	10.55	9.63
V/Cr	1.85	2.10	0.63	0.84	1.18	1.02	0.41	1.14	2.05	4.15	1.61	1.73
V/(V+Ni)	0.61	0.54	0.53	0.58	0.73	0.70	0.48	0.73	0.69	0.68	0.71	0.78

(To be continued on the next page)

(Continued)

Horizon	Guanyinqiao Formation					Longmaxi Formation						
Sample	Nbz28	Nbz29	Nbz30	Nbz31	Nbz32	Nbz33	Nbz34	Nbz35	Nbz36	Nbz37	Nbz38	Nbz39
Li	22.71	6.22	3.23	2.94	3.79	32.72	35.28	31.25	37.72	30.22	36.53	33.58
Be	2.56	0.76	0.53	0.48	0.56	2.49	3.78	2.68	1.80	2.25	2.49	2.50
Sc	11.36	2.65	1.46	1.20	2.27	13.15	16.16	12.33	8.82	10.23	12.12	10.84
V	119.76	24.38	16.58	14.81	20.04	1740.52	240.36	185.52	70.66	101.19	106.27	102.94
Cr	54.32	71.00	73.23	77.92	9.55	295.54	137.19	90.20	90.73	93.81	94.38	110.84
Co	10.20	4.03	2.75	2.95	2.67	14.07	20.69	13.79	7.13	7.86	10.28	11.06
Ni	46.34	50.36	52.52	56.82	14.82	214.58	102.97	54.88	23.03	22.23	28.38	30.06
Cu	18.76	6.16	1.95	7.13	1.52	143.50	44.77	39.47	15.16	21.72	21.15	19.76
Zn	53.06	69.80	56.51	61.08	15.59	696.08	156.67	125.07	93.94	67.71	70.03	39.59
Ga	14.99	3.24	2.19	1.85	2.26	19.18	25.19	19.56	14.03	16.37	18.45	18.84
Rb	136.50	29.63	17.23	14.24	20.48	146.08	226.99	165.84	111.65	132.13	156.62	144.42
Sr	250.20	561.81	341.68	331.25	210.86	94.03	76.43	127.80	143.24	122.66	130.22	128.36
Y	25.56	22.05	8.76	9.19	8.47	50.04	29.12	27.10	35.37	32.18	28.84	24.31
Zr	114.36	36.88	19.22	15.50	24.61	269.91	206.89	207.32	414.17	413.70	255.71	277.36
Nb	13.88	3.43	2.38	2.22	2.67	14.81	18.11	15.51	12.12	14.41	13.94	14.63
Cs	8.61	1.79	1.24	1.10	1.43	9.21	16.19	11.93	6.00	7.87	9.22	8.01
Ba	294.82	113.01	204.54	76.70	70.09	368.36	465.31	378.53	316.69	392.69	407.07	426.48
La	36.89	19.21	8.80	8.17	7.38	47.60	50.15	46.88	44.23	50.66	45.41	44.20
Ce	64.76	36.20	14.75	13.97	14.52	90.07	89.86	82.72	85.82	96.19	84.74	81.58
Pr	7.99	4.40	1.72	1.70	1.81	12.96	11.47	10.12	10.37	11.72	9.94	9.77
Nd	28.94	15.98	5.87	6.18	7.27	52.95	41.54	35.73	39.44	42.27	36.72	34.53
Sm	5.15	3.25	1.18	1.22	1.46	10.71	6.80	6.48	7.55	7.79	6.50	6.20
Eu	0.92	0.74	0.33	0.40	0.28	2.04	1.14	1.10	1.11	1.16	1.03	1.14
Gd	5.02	3.25	1.14	1.22	1.38	10.26	6.10	5.91	6.89	6.90	5.98	5.53
Tb	0.76	0.51	0.18	0.19	0.22	1.58	0.94	0.92	1.07	1.07	0.92	0.82
Dy	4.30	3.07	1.08	1.11	1.18	8.69	5.80	5.41	6.11	6.33	5.18	4.66
Ho	0.88	0.63	0.22	0.23	0.23	1.73	1.15	1.05	1.26	1.26	1.06	0.93
Er	2.39	1.69	0.63	0.65	0.62	4.48	3.24	2.88	3.48	3.39	2.93	2.55
Tm	0.35	0.25	0.10	0.10	0.10	0.61	0.49	0.43	0.52	0.51	0.43	0.38
Yb	2.25	1.54	0.63	0.61	0.63	3.75	3.21	2.74	3.32	3.32	2.71	2.51
Lu	0.32	0.23	0.09	0.09	0.09	0.56	0.50	0.41	0.50	0.50	0.41	0.39
Hf	3.28	1.06	0.53	0.40	0.66	7.97	6.11	6.11	12.07	11.56	7.60	7.96
Ta	1.31	0.23	0.14	0.12	0.16	1.16	1.96	1.62	0.97	1.38	1.12	1.52
Tl	0.87	0.29	0.16	0.16	0.17	3.76	6.50	2.98	0.85	0.89	1.02	0.93
Pb	16.96	5.79	2.63	3.70	3.24	19.50	46.65	36.24	16.86	21.95	21.74	20.94
Bi	0.24	0.06	0.03	0.04	0.04	0.33	0.74	0.44	0.18	0.31	0.26	0.26
Th	12.73	3.46	1.95	1.57	1.88	18.10	24.54	20.69	18.07	25.00	19.19	20.93
U	2.36	1.82	1.06	2.21	0.77	29.68	12.79	11.71	5.53	5.16	3.90	3.91
ΣREE	160.93	90.93	36.74	35.82	37.17	248.00	222.41	202.76	211.67	233.06	203.96	195.19
Ce/Ce*	0.82	0.86	0.82	0.82	0.87	0.79	0.82	0.83	0.87	0.86	0.87	0.86
Eu/Eu*	0.80	1.00	1.26	1.45	0.86	0.86	0.78	0.78	0.68	0.69	0.73	0.85
La _n /Yb _n	1.59	1.21	1.36	1.30	1.14	1.23	1.51	1.66	1.29	1.48	1.62	1.70
Ce/La	1.76	1.88	1.68	1.71	1.97	1.89	1.79	1.76	1.94	1.90	1.87	1.85
Th/U	5.39	1.90	1.84	0.71	2.44	0.61	1.92	1.77	3.27	4.85	4.93	5.36
V/Sc	10.54	9.20	11.39	12.36	8.85	132.39	14.87	15.05	8.01	9.89	8.77	9.50
V/Cr	2.20	0.34	0.23	0.19	2.10	5.89	1.75	2.06	0.78	1.08	1.13	0.93
V/(V+Ni)	0.72	0.33	0.24	0.21	0.57	0.89	0.70	0.77	0.75	0.82	0.79	0.77

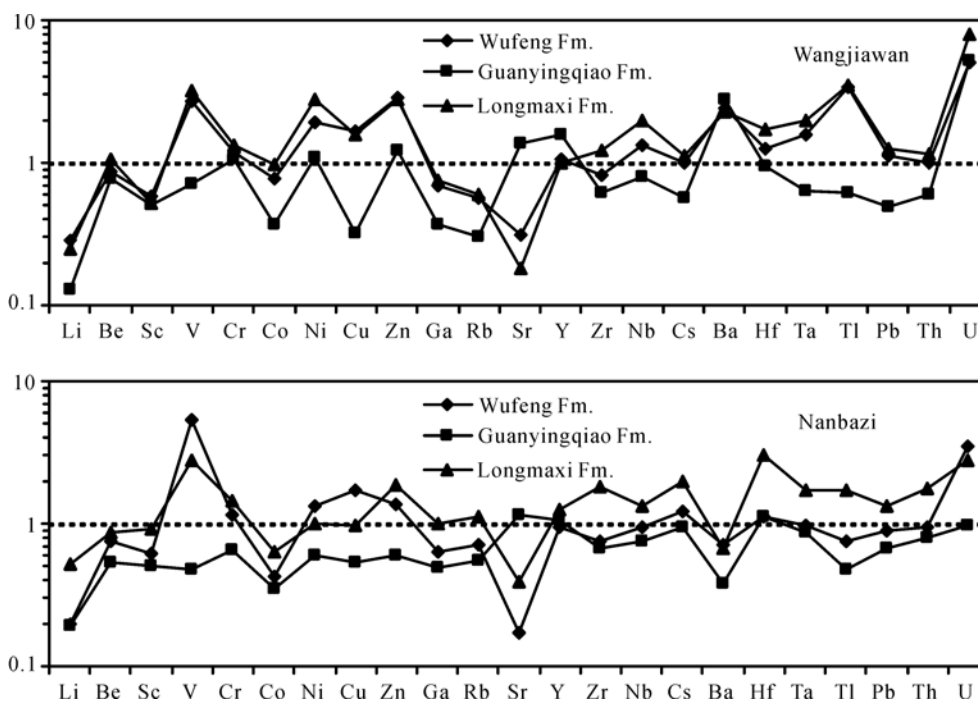


Figure 3 Trace element enrichment factors relative to average shale in sedimentary rocks of the Wangjiawan and Nanbazi sections.

as Li, Sc, Co, Ga, Rb and Sr are depleted. Both sections exhibit similarities in trace element abundance patterns displayed as $U > Zn > Ni > Ta > Nb > Pb > Be > Zr > Ga > Sc > Sr$ for black shales in the Wufeng Formation, as $Sr > Hf > Nb > Zr > Sc > Ga > Co > Li$ for the limestones and carbonaceous mudstones in the Guanyingqiao Formation, and as $U > V > Zn > Ta > Cr > Pb > Be > Co > Li > Sr$ for the black shales and silty mudstones in the Longmaxi Formation.

3.2 Rare earth elements (REE)

The REE data obtained from Wangjiawan and Nanbazi sections are listed in Tables 1 and 2, respectively. The total REE abundances (Σ REE) are variable, from 35.82 to 248.00 ppm (averaging 152.93 ppm) at Nanbazi section and from 63.42 to 496.74 ppm (averaging 176.77 ppm) at Wangjiawan section. Compared to the NASC standard, Σ REE in Nanbazi section are low in regimes greatly influenced by continental input, owing to the high sedimentation rate, which minimized exposure time to seawater and, thus, the adsorption of REE^[18,23]. However, Σ REE in Wangjiawan section are consistent with those of NASC, and reflect a more open and deep environment. Neither black shale nor carbonate samples from Wangjiawan section (Figure 4) exhibit significant deviations from flat REE patterns with an average $Ce/Ce^* = 0.88 \pm 0.08$ ($n=34$).

Normalized REE concentrations in black shale from

Wangjiawan section are thus similar to those in the common bulk shales widely reported elsewhere; however, REE distribution patterns of Nanbazi section samples (Figure 5), particularly carbonates, are anomalously depleted in Ce with an average $Ce/Ce^* = 0.84 \pm 0.13$ ($n=35$). At the Nanbazi section, Eu/Eu^* values display a negative anomaly in the Wufeng (averaging 0.83) and Longmaxi formations (averaging 0.77), but an unstable pattern varies from a slightly negative to positive anomaly in the Guanyingqiao Formation (averaging 0.87). A similar variation pattern of Eu/Eu^* values was also found at Wangjiawan section, with 0.51–1.03 (averaging 0.83) for the Wufeng Formation, 0.80–1.11 (averaging 0.98) for the Guanyingqiao Formation, and 0.74–1.03 (averaging 0.86) for the Longmaxi Formation. Generally, the Eu anomaly of Nanbazi section is less negative than that of Wangjiawan section.

4 Discussion

4.1 Trace element geochemistry

(1) Th/U ratios. The Th/U ratio has been used as a proxy for the redox condition of the depositional environment^[24,25]. Thorium is unaffected by redox conditions and remains insoluble as Th^{4+} . Uranium, however, exists as insoluble U^{4+} under highly reducing conditions, which leads to the U enrichment in sediments, whereas

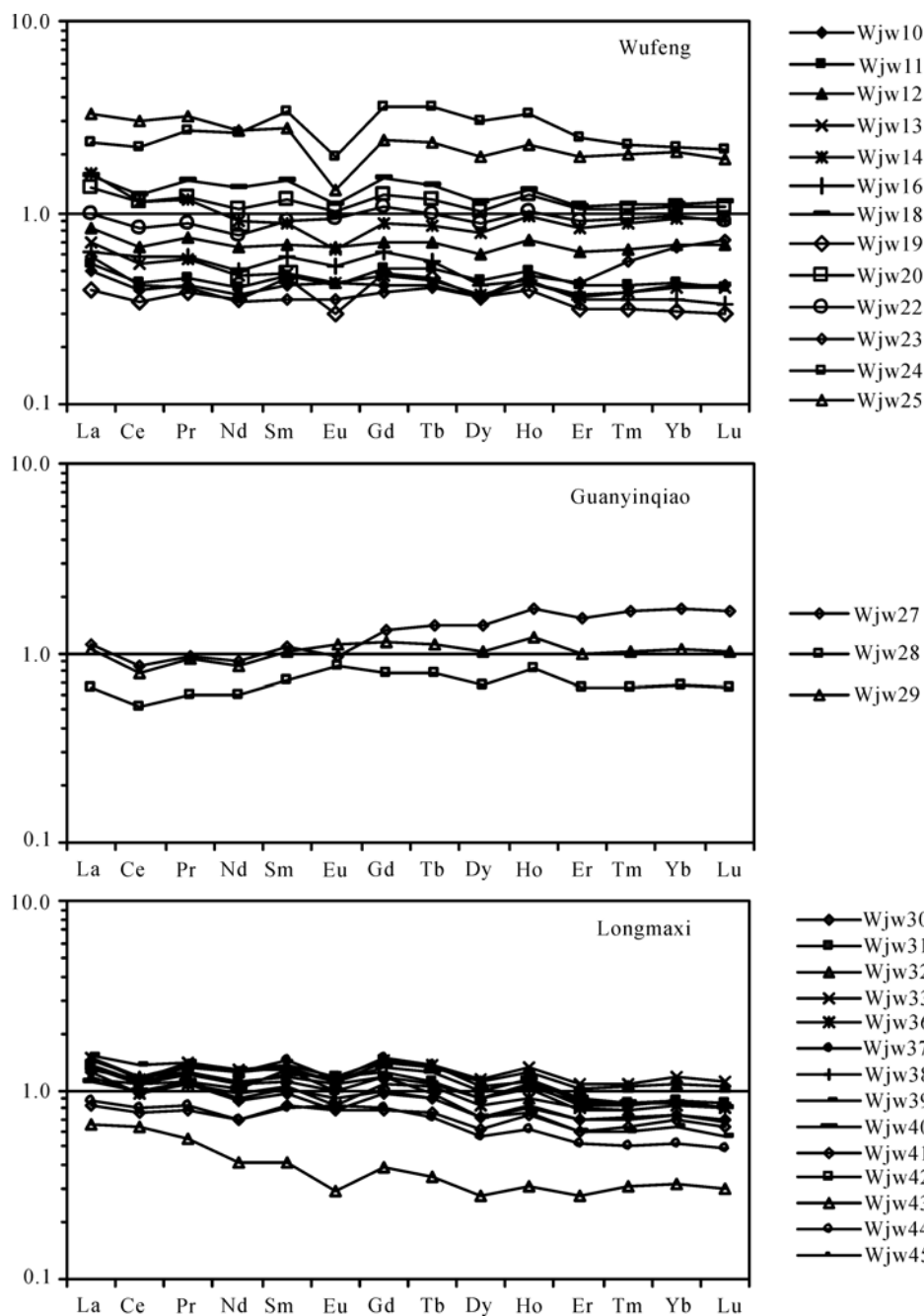


Figure 4 Shale-normalized REE distribution spectra of Late Ordovician-Early Silurian sedimentary rocks from the Wangjiawan section.

it exists as soluble U^{6+} under oxidizing conditions, leading to the U loss from sediments^[26]. Wignall and Twitchett^[27] suggested that environments characterized by anoxic conditions yielded Th/U ratios of 0 to 2 in the shale, and this criteria has been widely accepted in subsequent studies^[26,28].

Samples from Nanbazi section exhibit a wide range of Th/U ratios, oscillating from 0.58 to 5.39 (Figure 6), which suggests frequent fluctuations in environments from anoxic to oxic conditions through time. All sam-

ples from Wangjiawan section exhibit low Th/U ratios less than 2, with extreme Th/U ratios as low as 0.28 (Figure 6), this scenario suggests a more reducing environment at Wangjiawan compared with the data from Nanbazi section. It should be cautious when applying criteria established for paleoredox conditions^[29], as that, in this study, an anoxic condition inferred from those criteria for the Guanyinqiao Formation at Wangjiawan section is not consistent with the other evidence, i.e., extensive burrowings in the Guanyinqiao Formation^[27].

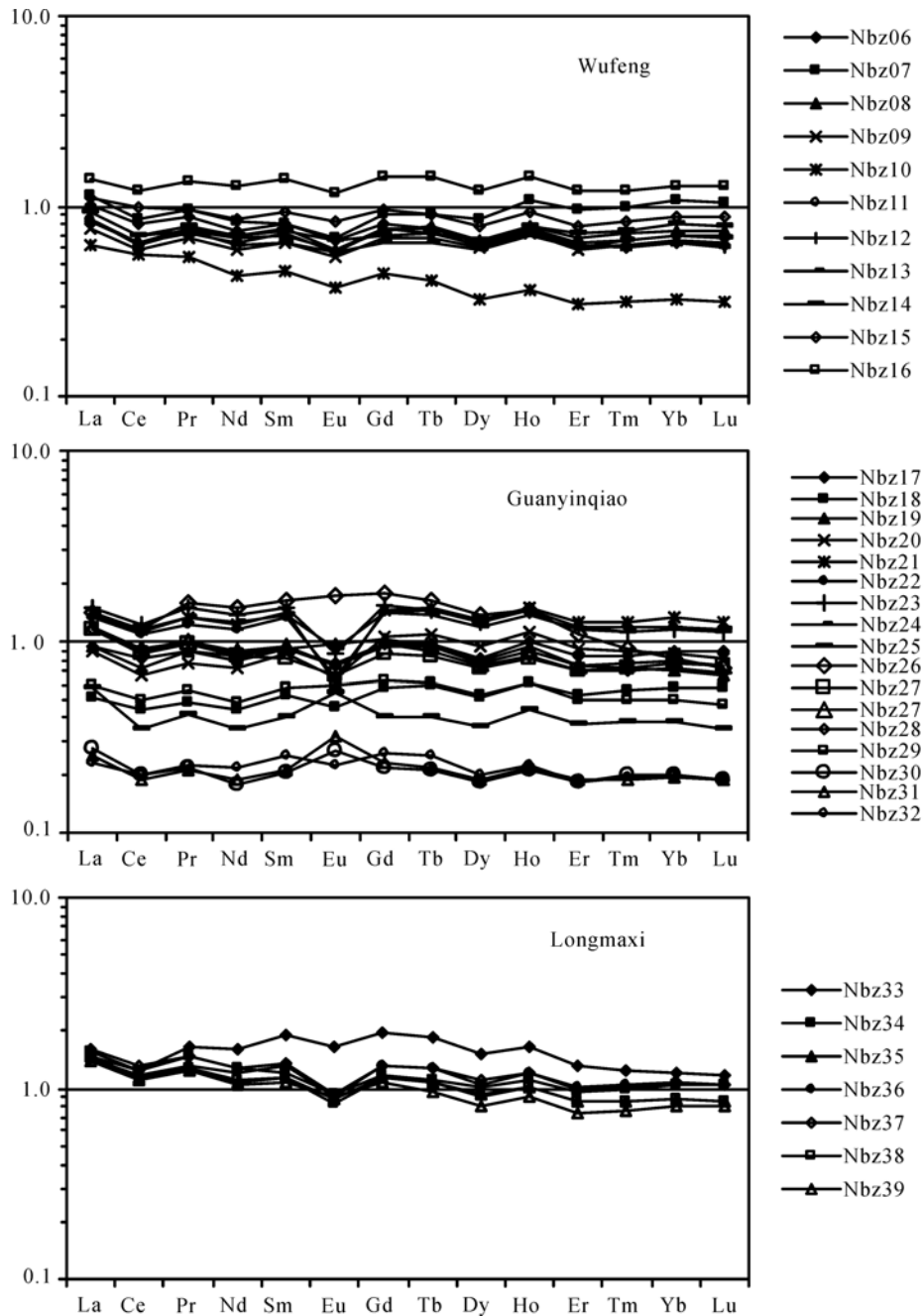


Figure 5 Shale-normalized REE distribution spectra of Late Ordovician-Early Silurian sedimentary rocks from the Nanbazi section.

Together with evidence of sedimentary facies and biota^[12], the Th/U ratios indicate anoxic conditions during Wufengian and Longmaxian intervals. An exception is found at the Upper Longmaxi Formation at Nanbazi section, where Th/U ratios yield higher values in the silty mudstone, suggesting more oxic bottom waters.

(2) Vanadium (V/Sc, V/Cr, V/(V+Ni)) systematics. Vanadium is also a redox-sensitive element that is preferentially concentrated in sediments underlying anoxic or near-anoxic waters^[29,30]. The degree of V enrichment

is most efficiently expressed if the V concentration is normalized by scandium abundance, because both V and Sc are insoluble and V varies in proportion to Sc, rather than to other insoluble elements such as Al and Ti^[26]. Kimura and Watanabe^[26] suggested that environments characterized by anoxic conditions resulted in significant V enrichment over Sc. Jones and Manning^[31] proposed that V/Cr ratios < 2 pointed to oxic conditions, 2–4.25 to dysoxic conditions, and > 4.25 to suboxic to anoxic conditions. Hatch and Leventhal^[32] demonstrated

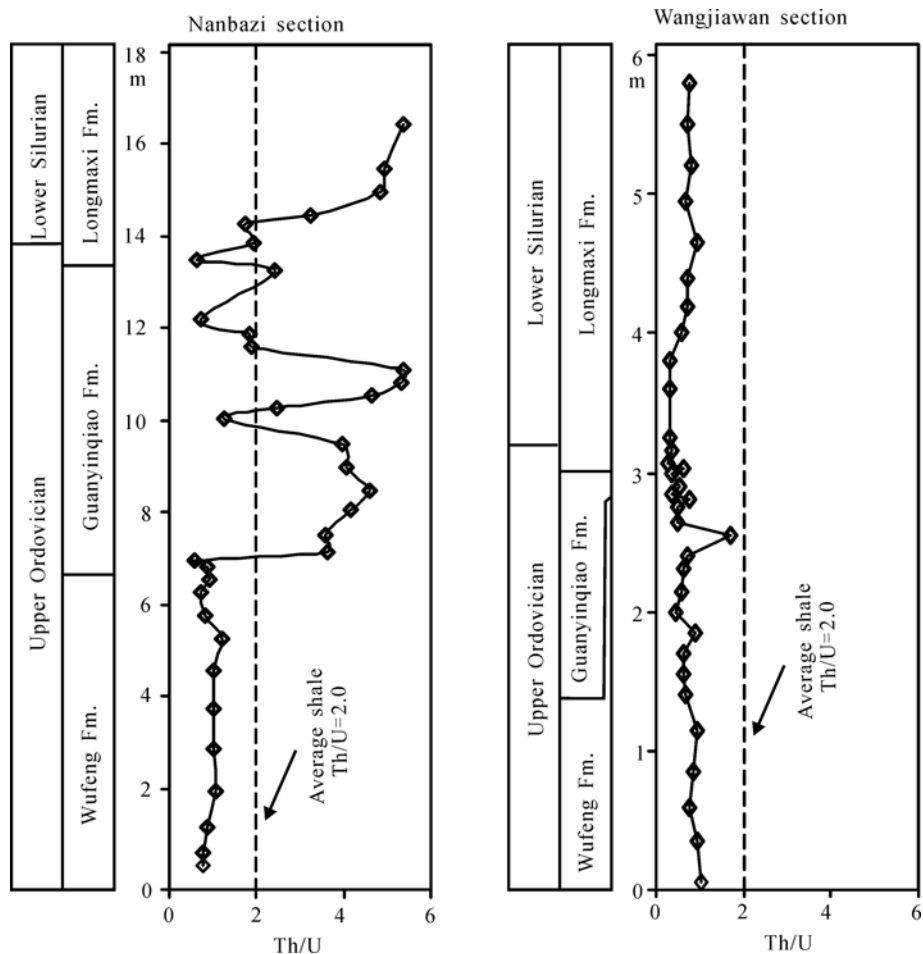


Figure 6 Th/U ratios of Late Ordovician-Early Silurian sedimentary rocks from the Wangjiawan and Nanbazi sections.

that $V/(V+Ni)$ ratios 0.46–0.60 for dysoxic conditions, 0.54–0.82 for anoxic conditions, and >0.84 for euxinic conditions. At Nanbazi section, our study showed that significant V enrichment over Sc (up to 171.52) occurred in samples that also exhibit Th/U ratios lower than 2, indicating anoxic bottom waters. Similar relationships were found in samples from Wangjiawan section, in which V/Sc ratio is as high as 115.01. In this study, a good agreement achieved in the interpretations of redox conditions derived from Th/U, V/Sc and $V/(V+Ni)$ ratios (Figure 7). However, V/Cr ratios point to a more oxic condition than either Th/U or $V/(V+Ni)$ ratios do for some Wufeng samples. For Guanyinqiao samples, V/Cr ratios indicate an oxic bottom water, which is consistent with the biotic evidence represented by well-developed benthic faunas, whereas Th/U and $V/(V+Ni)$ ratios point to a dysoxic to anoxic condition at Wangjiawan section, and an oxic to anoxic condition at Nanbazi section. Thus, it should be careful when applying these criteria to interpret the redox conditions.

4.2 Rare earth element (REE) systematics

Canet et al.^[33] suggested that the most distinctive features of the REE patterns of the shales are indicated by the slight enrichment in LREE, especially in Eu-La, and a conspicuous negative anomaly of Ce. In this study, the REE patterns are flat, indicating no apparent fractionation between the LREE and HREE, likely induced by anoxic conditions, except for a slight LREE depletion in the Guanyinqiao Formation at the Wangjiawan section (Figures 4, 5), probably resulted from a relatively oxic condition. Such patterns can be compared to those of the Upper Ordovician deposits from the South Uplands of Scotland^[18], which have essentially flat shale-normalized REE distribution patterns. The fact that REE patterns of shales from the same stratigraphic horizon are similar in different localities, even over a long distance, suggests that depositional environment on Yangtze Platform were uniform^[34]. This is consistent with the scenario of restricted, stagnant and stratified environment^[12].

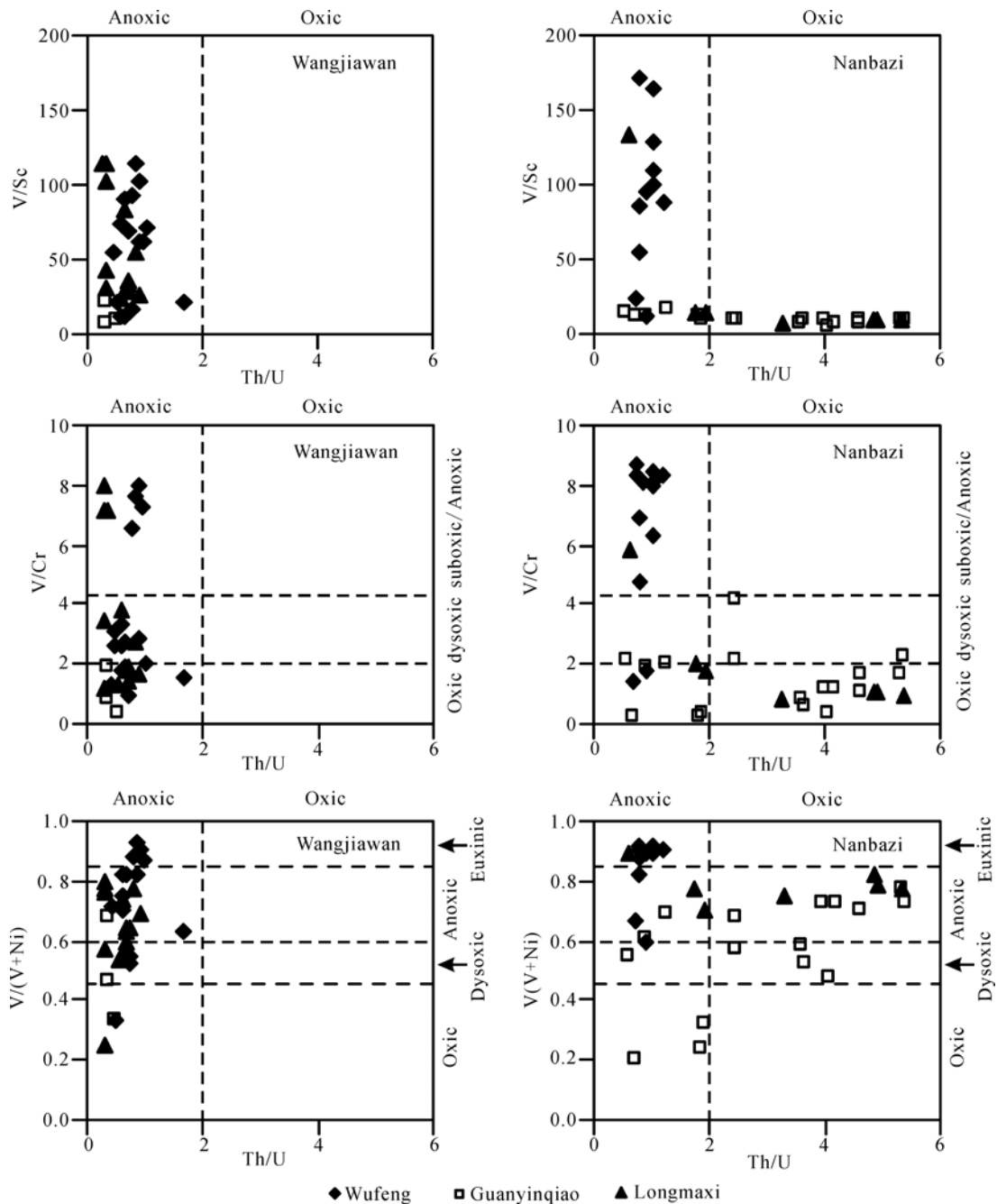


Figure 7 Crossplots of various trace-element ratios used as paleoredox proxies for the samples from Wangjiawan and Nanbazi sections.

(1) Ce anomaly. Normal seawater shows a marked depletion of Ce, owing to the predominance of oxidation to Ce^{4+} and accumulation in the sediments as CeO_2 . In contrast, at a local redox-cline such as that in the Black Sea, Ce is reduced to Ce^{3+} and the Ce anomaly disappears^[35]. Wright et al.^[36] and Wignall^[25] suggest that the Ce anomaly recorded the redox conditions of the overlying seawater column, and this signature remained in spite of subsequent burial and later diagenesis. The calculated Ce/Ce^* values of Wufeng Formation vary from

0.82 to 1.07 (averaging 0.88); those in the Guanyinqiao Formation range from 0.80 to 0.83 (averaging 0.81); and those in the lowermost of Longmaxi Formation from 0.81 to 1.05 (averaging 0.89). Generally, a low to moderate Ce depletion is recognized in the three stratigraphic intervals of the Wangjiawan section, but a slightly higher depletion in the Guanyinqiao Formation; this scenario implies a more reducing water column from which the black shales were deposited during the Wufengian and Longmaxian times. Similar secular

variations of Ce anomaly were also found for the samples from Nanbazi section, with 0.79–0.96 (averaging 0.85) for Wufeng Formation, 0.73–0.89 (averaging 0.82) for Guanyinqiao Formation, and 0.79–0.87 (averaging 0.84) for Longmaxi Formation.

(2) Eu anomaly. Eu anomalies have been reported in various types of igneous and sedimentary rocks^[37]. In many geological systems, Eu anomalies play a significant role in interpreting the physical and chemical conditions^[38–41]. The Eu/Eu* values are generally lower than 1, except for a few data greater than 1 in Guanyinqiao Formation, indicating negative anomalies in most cases. Those Eu/Eu* values greater than 1 may have been resulted from hydrothermal activity or extremely reducing conditions^[42,43]. Given the seabed was oxygenated during the Guanyinqiao period, as discussed above, positive Eu anomaly may be interpreted as a result of highly reducing hydrothermal fluids. If the positive Eu anomaly was derived from a hydrothermal source, then this hydrothermal signature must have been strongly modified by seawater because of the characteristic carbonate complexation signature of HREE depletion in the samples.

4.3 Palaeoenvironmental change and mass extinction

The available data on geochemical parameters in sediments are juxtaposed with stratigraphic intervals for which an associated anoxic event and/or a substantial biotic extinction have been claimed^[44]. Although Holsen^[45] suggested that there is not general association of Ce_{an} with other types of events, such as anoxic events or mass extinctions, Wang and Orth^[3] provided a sharp negative excursion of Ce_{an} clearly coincident with the Ordovician-Silurian boundary and mass extinctions. The increased concentrations of As, Sb and U in the eastern portions of the Yangtze Sea, at Jixian are interpreted as a reducing conditions at the *N.persculptus* zone at the base of Longmaxi Formation^[46], coinciding with the disappearance of benthic faunas as sea level rose and the seafloor became anoxic^[18]. In this study, the geochemical evidence suggests that the anoxic environment predominated over the Yangtze Platform during the Wufeng and Longmaxi intervals, and oxic bottom waters predominated over the Guanyinqiao interval. Patricka et al.^[34] suggested that changes between oxic and anoxic marine waters in one locality might occur in several

ways: (1) changes in water depth, (2) changes in organic productivity, and (3) changes in vertical stratification in upwelling or intensity of wind-driven marine currents. Although other factors cannot be ruled out, many researchers have proposed relative changes in sea level during this period^[1,7,12]. During the Guanyinqiao interval, sea level fell due to overgrowth of ice-sheet on land, and this led the seabed to be oxygenated on the Yangtze Platform. Once glaciation melted, sea level rose rapidly, and anoxic bottom waters extended over the Yangtze Platform. Moreover, increases of terrestrial influx into the ocean due to enhanced erosions may aggravate the eutrophic conditions, leading to more oxygen-depleted waters. The benthic organisms were immobile, having maximized external surfaces and passive circulatory systems, and they are highly sensitive to environmental changes in the ambient seawater^[47,48]. An oxygen deficiency lasting much longer than organism life spans is likely to have a significant impact on organisms^[26]. Persistence of environmental stress, related to redox changes, for a significant long period, could have resulted in the extinction of certain benthic organisms, i.e., *Hirnantia* fauna.

5 Conclusions

Based on these analyses of geochemical parameters for the Ordovician-Silurian sequence of the Yangtze Platform, the following may be concluded:

(1) Trace-element redox indices (especially Th/U, V/Sc, V/Cr and V/(V+Ni)) indicated anoxic conditions during the Wufeng and Longmaxi intervals, and an oxic condition during the Guanyinqiao interval. Nevertheless, cautions should be taken when applying these geochemical criteria.

(2) The positive Eu anomaly present in the Guanyinqiao Formation may have been derived from a hydrothermal source, but has been modified strongly by seawaters.

(3) The apparent stratigraphic coincidence between the biological demise and the oxygen-limited marine condition may imply a causal relationship between them. Oceanic anoxia could have played a significant role in the mass extinction during the Ordovician-Silurian transition.

We thank Feng Lianjun and Zhang Tonggang for their useful comments on the early manuscript. Thanks also go to Wang Zhuozhuo for field assistance, and to Jin Xindi for ICP-MS analysis.

- 1 Brenchley P J. Environmental changes close to the Ordovician-Silurian boundary. *Bull Br Mus Nat Hist (Geol)*, 1988, 43: 377–385
- 2 Marshall J D, Brenchley P J, Mason P, et al. Global carbon isotopic events associated with mass extinction and glaciation in the late Ordovician. *Palaeogeogr Palaeoclimatol Palaeoecol*, 1997, 132: 195–210[DOI]
- 3 Wang K, Orth C J. The great latest Ordovician extinction on the South China Plate: Chemostratigraphic studies of the Ordovician-Silurian boundary interval on the Yangtze Platform. *Palaeogeogr Palaeoclimatol Palaeoecol*, 1993, 104: 61–79[DOI]
- 4 Chen X, Rong J Y, Charles E M, et al. Late Ordovician to earliest Silurian graptolite and brachiopod biozonation from the Yangtze region, South China, with a global correlation. *Geol Mag*, 2000, 137(6): 623–650
- 5 Chen X, Rong J Y. Concepts and analysis of mass extinction with the Late Ordovician events as an example. *Hist Biol*, 1991, 5: 107–121
- 6 Wang K, Chatterton B D E, Wang Y. An organic carbon isotope record of Late Ordovician to Early Silurian marine sedimentary rocks, Yangtze Sea, South China: Implications for CO₂ changes during the Hirnantian glaciation. *Palaeogeogr Palaeoclimatol Palaeoecol*, 1997, 132: 147–158[DOI]
- 7 Berry W B N, Boucot A J. Glacio-eustatic control of Late Ordovician-Early Silurian platform sedimentation and faunal changes. *Geol Soc Am Bull*, 1973, 84: 275–284[DOI]
- 8 Stanley S M. Temperature and biotic crises in the marine realm. *Geology*, 1984, 12: 205–208[DOI]
- 9 Wilde P, Berry W B N. Destabilisation of the oceanic density structure and its significance to marine extinction events. *Palaeogeogr Palaeoclimatol Palaeoecol*, 1984, 48: 143–162[DOI]
- 10 Sheehan P M. Late Ordovician events and the terminal Ordovician extinction. *Bur Min Miner Resour Mem*, 1988, 44: 405–415
- 11 Goodfellow W D, Nowlan G S, McCracken A D, et al. Geochemical anomalies near the Ordovician-Silurian boundary, northern Yukon Territory, Canada. *Hist Biol*, 1992, 6: 1–23
- 12 Chen X, Rong J, Li Y, et al. Facies patterns and geography of the Yangtze region, South China, through the Ordovician and Silurian transition. *Palaeogeogr Palaeoclimatol Palaeoecol*, 2004, 204: 353–372[DOI]
- 13 Li J, Servais T, Yan K, et al. A nearshore-offshore trend in acritarch distribution from the Early-Middle Ordovician of the Yangtze Platform, South China. *Rev Palaeobot Palynol*, 2004, 130: 141–161[DOI]
- 14 Wang H Z. Atlas of the Palaeogeography of China (in Chinese). Beijing: Cartographic Publishing House, 1985
- 15 Cocks L R M. Ordovician and Silurian global geography. *Geol Soc London J*, 2001, 158: 197–210
- 16 Ma L, Chen Y J, Gan K W, et al. Geotectonic Geology of Southern China and Marine Petroleum Geologic Characteristics (in Chinese). Beijing: Geological Publishing House, 2004
- 17 Wang X F, Chai Z F. Ordovician-Silurian boundary extinction and its relationship to iridium and carbon isotope anomalies (in Chinese). *Acta Geol Sin*, 1989, 3: 255–263
- 18 Zhang T S, Kershaw S, Wan Y, et al. Geochemical and facies evidence for palaeoenvironmental change during the Late Ordovician Hirnantian glaciation in South Sichuan Province, China. *Glob Planet Change*, 2000, 24: 133–152[DOI]
- 19 Taylor S R, McLennan S M. *The Continental Crustal: Its Composition and Evolution*. Oxford: Blackwell, 1985
- 20 Sholkovitz R E. Rare earth elements of the North Atlantic Ocean, Amazon Delta, and East China Sea: Reinterpretation of terrigenous input patterns to the ocean. *Am J Sci*, 1988, 288: 236–281
- 21 Murray R W, Buchholtz M R, Gerlach D C, et al. Rare earth, major, and trace elements in chert from the Franciscan complex and Monterey group, Californian: Assessing REE sources to fine-grained marine sediments. *Geochim Cosmochim Acta*, 1991, 55: 1875–1895[DOI]
- 22 Murray R W. Chemical criteria to identify the depositional environment of chert: General principles and applications. *Sediment Geol*, 1994, 90: 213–232[DOI]
- 23 Owen A W, Armstrong H A, Floyd J D. Rare earth element geochemistry of upper Ordovician cherts from the Southern Upland of Scotland. *J Geol Soc*, 1999, 156: 191–204[DOI]
- 24 Myers K J, Wignall P B. Understanding Jurassic organic-rich mudrocks — New concepts using gamma ray spectrometry and palaeoecology: Examples from the Kimmeridge clay of Dorset and the Jet rock of Yorkshire. In: Leggett J K, Zuffa G G, eds. *Marine Clastic Sedimentology*. London: Graham and Trotman, 1987. 1–45
- 25 Wignall P B. *Black Shales*. New York: Oxford University Press, 1994
- 26 Kimura H, Watanabe Y. Ocean anoxia at the Precambrian-Cambrian boundary. *Geology*, 2001, 29: 995–998[DOI]
- 27 Wignall P B, Twitchett R J. Oceanic anoxia and the end Permian mass extinction. *Science*, 1996, 272: 1155–1158[DOI]
- 28 Guo Q J, Shields G A, Liu C Q, et al. Trace element chemostratigraphy of two Ediacaran-Cambrian successions in South China: Implications for organosedimentary metal enrichment and silicification in the early Cambrian. *Palaeogeogr Palaeoclimatol Palaeoecol*, 2007, 254: 194–216[DOI]
- 29 Rimmer S M. Geochemical paleoredox indicators in Devonian-Mississippian black shales, central Appalachian Basin (U.S.A.). *Chem Geol*, 2004, 206: 373–391[DOI]
- 30 Emerson S R, Huested S S. Ocean anoxia and the concentrations of molybdenum and vanadium in seawater. *Mar Chem*, 1991, 34: 177–196[DOI]
- 31 Jones B, Manning D A C. Comparison of geochemical indices used for the interpretation of palaeoredox conditions in ancient mudstones. *Chem Geol*, 1994, 111: 111–129[DOI]
- 32 Hatch J R, Leventhal J S. Relationship between inferred redox potential of the depositional environment and geochemistry of the Upper Pennsylvanian (Missourian) stark shale member of the Dennis Limestone, Wabaunsee County, Kansas, USA. *Chem Geol*, 1992, 99: 65–82[DOI]
- 33 Canet C, Alfonso P, Melgarejo J C, et al. Geochemical evidences of sedimentary-exhalative origin of the shale-hosted PGE-Ag-Au-Zn-Cu occurrences of the Prades Mountains (Catalonia, Spain): Trace element abundances and Sm-Nd isotopes. *J Geochem Expl*, 2004, 82: 17–33[DOI]
- 34 Patricka D, Martin J E, Parris D C, et al. Paleoenvironmental interpretations of rare earth element signatures in mosasaurs (reptilia) from the upper Cretaceous Pierre Shale, central South Dakota, USA. Pa-

- laeogeogr Palaeoclimatol Palaeoecol, 2004, 212: 277–294
- 35 Rasmussen B, Buick R, Taylor W R. Removal of oceanic REE by authigenic precipitation of phosphatic minerals. *Earth Planet Sci Lett*, 1998, 164: 135–149[[DOI](#)]
- 36 Wright J, Schrader H, Holser W T. Paleoredox variations in ancient oceans recorded by rare earth elements in fossil apatite. *Geochim Cosmochim Acta*, 1987, 51: 631–644[[DOI](#)]
- 37 Henderson P. *Rare Earth Element Geochemistry*. Amsterdam: Elsevier, 1984
- 38 Derry L A, Jacobsen S B. The chemical evolution of Precambrian seawater: Evidence from REEs in banded iron formations. *Geochim Cosmochim Acta*, 1990, 49: 1955–1963
- 39 Lee S G, Kima Y, Chae B, et al. The geochemical implication of a variable Eu anomaly in a fractured gneiss core: Application for understanding Am behavior in the geological environment. *Appl Geochem*, 2004, 19: 1711–1725[[DOI](#)]
- 40 Fedo C M, Eriksson K A, Krogstad E J. Geochemistry of shales from the Archean (~3.0 Ga) Buhwa Greenstone Belt, Zimbabwe: Implications for provenance and source-area weathering. *Geochim Cosmochim Acta*, 1996, 60: 1751–1763[[DOI](#)]
- 41 Sugitani K, Yamashita F, Nagaoka T, et al. Geochemistry and sedimentary petrology of Archean clastic sedimentary rocks at Mt. Goldsworthy, Pilbara Craton, Western Australia: Evidence for the early evolution of continental crust and hydrothermal alteration. *Precambrian Res*, 2006, 147: 124–147[[DOI](#)]
- 42 MacRae N D, Nesbitt H W, Kronberg B I. Development of a positive Eu anomaly during diagenesis. *Earth Planet Sci Lett*, 1992, 109: 585–591[[DOI](#)]
- 43 Kidder D L, Krishnaswamy R, Mapes R H. Elemental mobility in phosphatic shales during concretion growth and implications for provenance analysis. *Chem Geol*, 2003, 198: 335–353[[DOI](#)]
- 44 Saltzman M R, Davidson J P, Holden P, et al. Sea-level-driven changes in ocean chemistry at an Upper Cambrian extinction horizon. *Geology*, 1995, 23: 893–896[[DOI](#)]
- 45 Holser W T. Evaluation of the application of rare-earth elements to paleoceanography. *Palaeogeogr Palaeoclimatol Palaeoecol*, 1997, 132: 309–323[[DOI](#)]
- 46 Wang K, Chatterton B D E, Attrep M J, et al. Iridium abundance maxima at the latest Ordovician mass extinction horizon, Yangtze Basin, China: Terrestrial or extraterrestrial? *Geology*, 1992, 20: 39–42[[DOI](#)]
- 47 Seilacher A. Vendobionta and Psammocorallia: Lost constructions of Precambrian evolution. *Geol Soc London J*, 1992, 149: 607–613[[DOI](#)]
- 48 Brasier M D. The basal Cambrian transition and Cambrian bio-events (from terminal Proterozoic extinctions to Cambrian biomes). In: Walliser O H, ed. *Global Events and Event Stratigraphy in the Phanerozoic*. Berlin: Springer-Verlag, 1995. 11–28